

See discussions, stats, and author profiles for this publication at: <https://www.researchgate.net/publication/7011173>

Fabrication and Characterization of Molecular Beam Epitaxy Grown Thin-Film GaAs Waveguides for Mid-Infrared Evanescent Field Chemical Sensing

ARTICLE *in* ANALYTICAL CHEMISTRY · JULY 2006

Impact Factor: 5.64 · DOI: 10.1021/ac052214a · Source: PubMed

CITATIONS

40

READS

63

4 AUTHORS, INCLUDING:



Jérôme Faist

ETH Zurich

687 PUBLICATIONS 19,024 CITATIONS

SEE PROFILE



Boris Mizaikoff

Universität Ulm

311 PUBLICATIONS 4,800 CITATIONS

SEE PROFILE

Fabrication and Characterization of Molecular Beam Epitaxy Grown Thin-Film GaAs Waveguides for Mid-Infrared Evanescent Field Chemical Sensing

Christy Charlton,[†] Marcella Giovannini,[‡] Jérôme Faist,[‡] and Boris Mizaikoff^{*,†}

School of Chemistry and Biochemistry, Georgia Institute of Technology, Atlanta, Georgia 30332-0400, Institute of Physics, University of Neuchâtel, Rue A-L. Breguet 1 CH-2000 Neuchâtel, France

Thin-film GaAs waveguides were designed and fabricated by molecular beam epitaxy for use in mid-infrared (MIR) evanescent field liquid sensing. Waveguides were designed to facilitate the propagation of a single mode at a wavelength of 10.3 μm emitted from a distributed feedback quantum cascade laser, which overlaps with molecular selective absorption features of acetic anhydride. The characterization of the waveguides shows transmission across a broad MIR band. Evanescent field absorption measurements indicate a significant sensitivity enhancement in contrast to multimode planar silver halide waveguides.

The mid-infrared (MIR, 2–20 μm) spectral band is particularly useful for sensing applications due to the excitation of fundamental rotational and vibrational transitions¹ allowing for sensitive and selective detection of the molecules in the gas and liquid phase. For liquid sensing, attenuated total reflection² and evanescent field absorption measurements facilitate probing of samples that are too opaque for transmission absorption measurements such as in environmental monitoring,^{3,4} process analysis,⁵ and biological applications.^{6,7}

If total internal reflection occurs, an evanescent field extends at the interface between the optically denser waveguide (refractive index n_1) and an optically thinner adjacent medium (refractive index n_2 ; with $n_1 > n_2$).⁸ The penetration depth, d_p , of the evanescent field is defined as

$$d_p = \lambda / 2\pi(n_1^2 \sin^2 \theta - n_2^2)^{1/2}$$

where λ is the wavelength of the radiation and θ is the incoupling angle. Absorbing species present within the penetration depth of the evanescent field interact with radiation, resulting in attenuation of the frequencies where resonant energy transfer to the vibrational modes of molecules occurs.

As the intensity of the evanescent field strongly depends on the waveguide geometry,^{9–11} decreasing the fiber diameter or tapering a section of the fiber increases the intensity of the evanescent field and thereby improves the sensitivity to absorbing species at or close to the waveguide surface.^{12–15} Evanescent field absorption measurements follow a pseudo Lambert–Beer relationship, where the absorbance A is defined as

$$A = (\epsilon Cl)r$$

where ϵ is the molar absorptivity, C is the concentration, l is the optical path length, and r is the fraction of power guided outside the waveguide core. Maximum evanescent field intensity, and therefore a maximum value of r , would occur in a single-mode waveguide, which is thickness-matched to the emission frequency of a corresponding laser light source. Ideal optimization conditions are limited to mono-mode laser light sources providing a platform for highly integrated MIR evanescent field sensing systems.

Laser light sources provide enhanced spectral density compared to conventional broadband MIR sources. Consequently, if a narrow emission band is matched to a carefully selected absorption band characteristic for the analyte of interest, sufficient selectivity but higher sensitivity can be achieved in a more compact and miniaturizable sensing system.

* To whom correspondence should be addressed: (phone) 404-894-4030; (Fax) 404-385-6447; (e-mail) boris.mizaikoff@chemistry.gatech.edu; (URL) <http://asl.chemistry.gatech.edu>.

[†] Georgia Institute of Technology.

[‡] University of Neuchâtel.

(1) Mizaikoff, B. *Anal. Chem.* **2003**, *75*, 258A–267A.

(2) Fahrenfort, J. *Spectrochim. Acta* **1961**, *17*, 698–709.

(3) Kraska, R.; Taga, K.; Kellner, R. *Appl. Spectrosc.* **1993**, *47*, 1484–1587.

(4) Karlowatz, M.; Kraft, M.; Mizaikoff, B. *Anal. Chem.* **2004**, *76*, 2643–2648.

(5) Janotta, M.; Vogt, F.; Voraberger, H.; Waldhauser, W.; Lackner, J. M.; Stotter, C.; Beutl, M.; Mizaikoff, B. *Anal. Chem.* **2004**, *76*, 384–391.

(6) Taga, K.; Kellner, R.; Kainz, U.; Sleytr, U. B. *Anal. Chem.* **1994**, *66*, 35–39.

(7) Plunkett, S. E.; Jonas, R. E.; Braiman, M. S. *Biophys. J.* **1997**, *73*, 2235–2240.

(8) Harrick, N. J. *Internal Reflection Spectroscopy*; Wiley: New York, 1967.

(9) Simhony, S.; Schnitzer, I.; Katzir, A.; Kosower, E. M. *J. Appl. Phys.* **1988**, *64*, 3732–3734.

(10) Messina, A.; Greenstein, A.; Katzir, A. *Appl. Opt.* **1996**, *35*, 2274–2284.

(11) Ruddy, V.; MacCraith, B. D.; Murphy, J. A. *J. Appl. Phys.* **1990**, *67*, 6070–6074.

(12) Plunkett, S. E.; Propst, S.; Braiman, M. S. *Appl. Opt.* **1997**, *36*, 4055–4061.

(13) MacDonald, S.; Michel, K.; LeCoq, D.; Boussard-Pledel, C.; Bureau, B. *Opt. Mater.* **2004**, *25*, 171–178.

(14) Raichlin, Y.; Fel, L.; Katzir, A. *Opt. Lett.* **2003**, *28*, 2297–2299.

(15) Vongsvivut, J.; Shilov, S.; Ekgasit, S.; Braiman, M. *Appl. Spectrosc.* **2002**, *56*, 1552–1561.

Quantum cascade lasers (QCLs)¹⁶ have successfully been applied in sensing formats due to their wide coverage of MIR emission frequencies^{17–19} and have recently demonstrated their suitability for evanescent field MIR sensing.^{20,21} Distributed feedback (DFB) QCLs provide narrow emission line width ($\sim 0.006 \text{ cm}^{-1}$)²² by incorporating a grating exposed²³ or buried²⁴ at the surface of the laser ridge, thus facilitating the selection of overlapping analyte bands.

Infrared transmitting fibers²⁵ are fabricated from materials such as polycrystalline silver halides, amorphous chalcogenide glasses, single-crystal sapphire, fluoride glasses, and tellurium halides. Silver halides^{4,5,9,20} and chalcogenide glasses¹³ are the predominant materials for MIR liquid-phase fiber-optic sensing applications.¹

The present study demonstrates MIR evanescent field sensors with a new generation of GaAs thin-film planar waveguides designed and fabricated to match the emission band of a QCL light source. These single-mode IR waveguides are designed to improve the sensitivity of evanescent field absorption measurements and to provide a platform for the development of a highly integrated and miniaturized MIR liquid-phase sensing system aimed at incorporating QCL and waveguide on a single chip. The GaAs material has the advantage of exhibiting very low absorption across the whole mid-infrared to a wavelength of $16 \mu\text{m}$ where the first multiphonon absorption features are present. The reststrahlen band will completely eliminate radiation at approximately $\lambda = 25\text{--}40 \mu\text{m}$.²⁶ Low loss waveguides can be epitaxially grown utilizing the relatively large refractive index step between $\text{Al}_x\text{Ga}_{1-x}\text{As}$ and GaAs materials.

EXPERIMENTAL SECTION

Chemicals. Acetic anhydride was purchased from Sigma Aldrich (Milwaukee, WI) at 99.9% purity, and acetonitrile was obtained from VWR (West Chester, PA) at HPLC grade.

Waveguide Fabrication. Waveguides were fabricated by molecular beam epitaxy on a Si-doped GaAs wafer substrate. The doped substrate was selected to effectively absorb and thereby suppress stray light occurring outside the optical waveguide, as its free carrier absorption is over 300 cm^{-1} at $\lambda = 974 \text{ cm}^{-1}$. The waveguide consisted of a $6\text{-}\mu\text{m}$ $\text{Al}_{0.2}\text{Ga}_{0.8}\text{As}$ cladding layer, followed by a $6\text{-}\mu\text{m}$ GaAs core layer that completed the epitaxial growth. To passivate the surface against potential etching or corrosion by the sample solution being sensed, a 300-nm Si_3N_4 layer was deposited by PECVD at the surface of some waveguide samples.

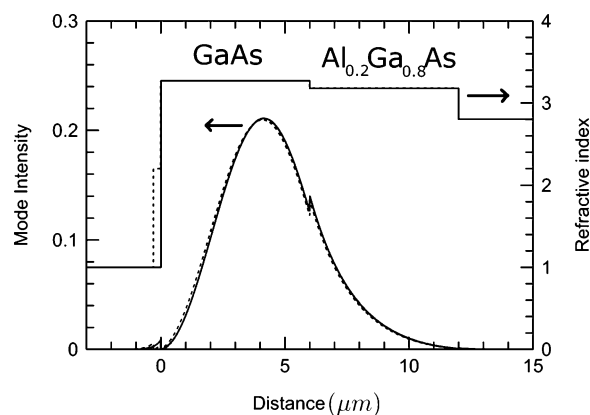


Figure 1. Computed optical mode profile. Refractive index profile (right axis) and optical mode profile (left axis) for a waveguide without silicon nitride overlayer.

A schematic of the refractive index distribution of the waveguide structure and a computed optical mode profile for TM polarized light is displayed in Figure 1. The computed overlap of the evanescent field with a gaseous species (assuming $n = 1$) is 2.3×10^{-3} , decreasing to 1.6×10^{-3} with the additional Si_3N_4 overlayer. In the presence of a liquid with a higher refractive index, the overlap value increases accordingly. Larger overlap is achieved for more tightly confined waveguides, however, with the compromise of a large numerical aperture for the mode. The computed waveguide absorption is only 0.27 cm^{-1} , which is limited by leakage of the mode inside the $n+$ doped substrate. This low value of losses enables the application of single-mode planar waveguides with a length of a few centimeters at yet acceptable losses.

Finally, processed wafers were cleaved into strip waveguides by scoring along the crystal axis with a diamond knife and breaking along the score. The waveguides were each 0.5 cm wide and varied in length from 1 to 2.5 cm . The optical quality of the end facets was verified by scanning electron microscopy. FT-IR spectra were recorded at strip waveguides with a length of 1 cm and a width of 0.5 cm .

FT-IR Measurements. Coupling into waveguide segments was achieved by focusing the collimated unpolarized beam from a FT-IR spectrometer (Bruker IFS 66, Bruker Optics, Billerica, MA) onto the waveguide end facet using an off-axis parabolic mirror with a focal length of 3 in . Light emanating from the distal end of the waveguide was collected by pigtail coupling of the waveguide to the ZnSe window of a liquid nitrogen cooled MCT detector (Kolmar Technologies, Newburyport, MA).

QCL Measurements. Evanescent field measurements with GaAs waveguides were demonstrated by coupling with a DFB-QCL (Alpes Lasers, Neuchatel, Switzerland) emitting TM polarized light at 974 cm^{-1} ($10.3 \mu\text{m}$), which overlaps with the $\text{CH}_3\text{--C}$ bending vibration of acetic anhydride.²⁰ The laser was operated at a temperature of 10°C and modulated at a pulse duration of 40 ns with a period of $2.64 \mu\text{s}$. During the pulse, the amplitude was controlled by an external power supply set to 22 V . The QCL was pigtail coupled to the waveguide as shown in Figure 2. Radiation from the distal end of the waveguide was collected by a MCT detector, similar to the FT-IR experiments.

Acetic anhydride was deposited at the waveguide surface in $0.5\text{-}\mu\text{L}$ droplets, each covering a length of 3 mm at the center of the waveguide surface as shown in Figure 2. Sequential addition

- (16) Faist, J.; Capasso, F.; Sirtori, C.; Sivco, D. L.; Hutchinson, A. L.; Cho, A. Y. *Science* **1994**, *264*, 553–558.
- (17) Kosterev, A.; Tittel, F. *IEEE J. Quantum Electron.* **2002**, *38*, 582–591.
- (18) Gmachl, C.; Capasso, F.; Sivco, D. L.; Cho, A. Y. *Rep. Prog. Phys.* **2001**, *64*, 1533–1601.
- (19) Charlton, C.; Temelkuran, B.; Dellemann, G.; Mizaikoff, B. *Appl. Phys. Lett.* **2005**, *86*, 194102–194104.
- (20) Charlton, C.; Katzir, A.; Mizaikoff, B. *Anal. Chem.* **2005**, *77*, 4398–4403.
- (21) Chen, J. Z.; Liu, Z.; Gmachl, C. F.; Sivco, D. L. *Opt. Express* **2005**, *13*, 5953–5960.
- (22) Zahniser, M. S.; Fraunhofer IPM QC Laser Workshop, 2001.
- (23) Faist, J.; Gmachl, C.; Capasso, F.; Sirtori, C.; Sivco, D. L.; Baillargeon, J. N.; Cho, A. Y. *Appl. Phys. Lett.* **1997**, *70*, 2670–2672.
- (24) Gmachl, C.; Faist, J.; Baillargeon, J. N.; Capasso, F.; Sirtori, C.; Chu, S. N. G.; Cho, A. Y. *IEEE Photonics Technol. Lett.* **1997**, *9*, 1090–1092.
- (25) Harrington, J. A. *Infrared Fibers and Their Applications*, 1st ed.; SPIE Press: Bellingham, WA, 2004.
- (26) Palik, E. D., Ed. *Handbook of optical constants of solids*; Academic Press: New York, 1985.

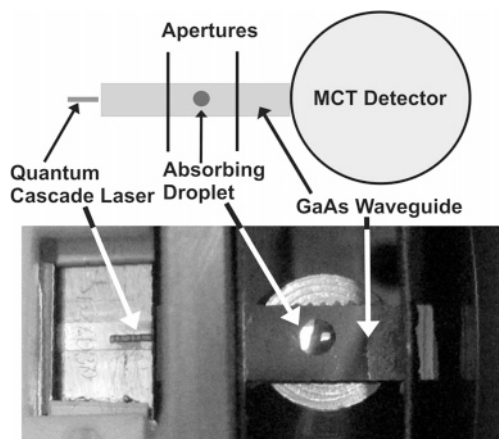


Figure 2. QCL coupled to GaAs waveguide. Experimental setup for QCL-based evanescent field absorption measurements with the QCL pigtail coupled to a GaAs waveguide and a droplet of absorbing analyte at the waveguide surface.

of two more droplets of the same volume and surface area increased the covered waveguide surface area, thereby generating a response curve corresponding to the change in light intensity through the waveguide (I/I_0) as a function of the absorbing analyte coverage length along the waveguide surface. For comparison, the evanescent field absorption measurements were repeated at the surface of a multimode silver halide planar waveguide with a thickness of $300\ \mu\text{m}$ (width, $3\ \text{mm}$; length, $35\ \text{mm}$). Light was coupled into the silver halide waveguide at or near the critical angle resulting in the most sensitive evanescent field measurements achievable with this waveguide.

Acetonitrile, which does not absorb at the $10.3\text{-}\mu\text{m}$ emission wavelength of the QCL²⁰ was also deposited at the surface of both waveguides verifying no damping of the laser radiation due to the solvent. Hence, it was confirmed that the signal change in the case of acetic anhydride deposition exclusively results from molecule-specific absorption rather than, for example, refractive index modulation effects.

RESULTS AND DISCUSSION

Figure 3 shows single-beam FT-IR transmission spectra recorded by coupling radiation through the long axis of different waveguides with and without silicon nitride overlayer, respectively. For reference, a detector response curve without waveguide is provided. All spectra show characteristic gaseous CO_2 features at $\sim 2300\ \text{cm}^{-1}$, and water vapor bands at ~ 1600 and $\sim 3700\ \text{cm}^{-1}$ resulting from the ambient environment. The spectra recorded through the waveguides are characterized by much lower signal-to-noise ratios, due to the comparatively small amount of radiation coupled into these thin-film planar waveguide structures. It is evident that, besides the decrease in transmitted light energy, no change of the spectral transmission window is occurring in comparison between the GaAs waveguide and the detector response curve. These spectra reveal that despite being optimized to transmit light at $10.3\ \mu\text{m}$, broadband IR light is still propagated by the waveguide. However, the spectra for the waveguide overcoated with silicon nitride clearly reveal solid-state absorption features centered at $2150\ \text{cm}^{-1}$ and a shifted transmission cutoff wavelength at $1250\ \text{cm}^{-1}$ resulting from the additional Si_3N_4 layer.

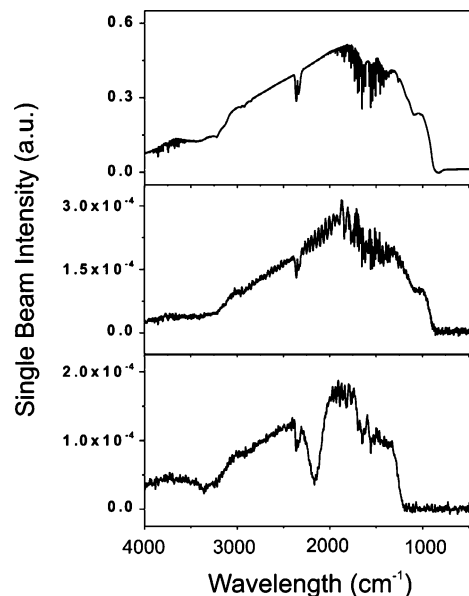


Figure 3. FT-IR transmission spectra of GaAs waveguides. FT-IR spectra recorded with (top) no waveguide, (middle) a GaAs waveguide, and (bottom) a GaAs waveguide with silicon nitride overlayer.

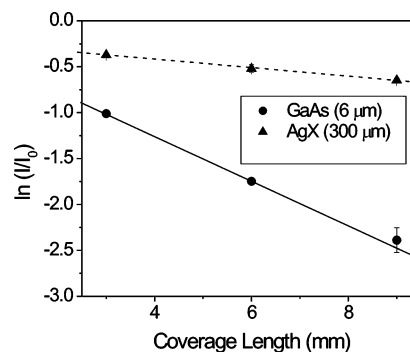


Figure 4. Response curve. System response for GaAs waveguide (●) and silver halide (AgX) waveguide (▲) as a function of the waveguide surface coverage area along with linear regression fits.

Response curves for both waveguides are shown in Figure 4; the circular symbols represent the response obtained with the GaAs waveguide fitted with a linear regression function (solid line). The response for the silver halide waveguide is indicated with triangular symbols and a dashed linear regression fit. In comparing the slopes of the two linear fits, it is shown that the GaAs response function has a slope of 0.24, while the slope of the response function for the silver halide waveguide is 0.05. Hence, an improvement in evanescent field sensitivity by a factor of 5 is clearly evident for the single-mode GaAs waveguide. This increase in sensitivity obtained from the thin-film GaAs waveguide is attributed to an increase in r , which is the fractional radiation power guided outside the core of the single-mode waveguide. In this context, it should be considered that the current waveguide structure is optimized for low loss rather than maximum overlap. Hence, it is expected that by increasing r an improved sensitivity by 1 order of magnitude or more can be achieved.

The theoretical change in transmission achievable with the GaAs waveguide was calculated at 0.803 using the Lambert–Beer law based on an extinction coefficient for acetic anhydride of $2.69\ \text{L/mol}\cdot\text{mm}$. This value was obtained from IR transmission spectroscopy of the pure analyte recorded at an optical path length

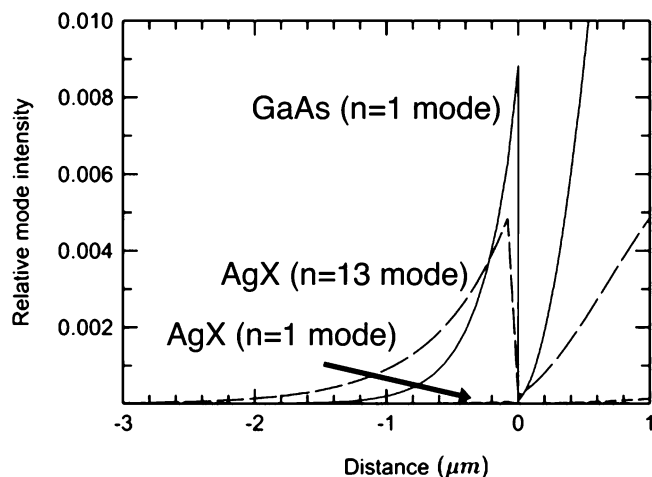


Figure 5. Mode profiles. Relative mode intensity for TM polarized light as a function of distance perpendicular to the direction of propagation for GaAs fundamental mode (solid), AgX high-order mode (long dash), and AgX fundamental mode (short dash) with the region <0 located outside the waveguide (evanescent field).

of 3 mm, which corresponds to the diameter of a single droplet deposited at the waveguide surface, and a fractional evanescent field power of 2.3×10^{-3} . The experimentally obtained value for a single droplet at the GaAs waveguide surface is 0.638. The difference between the calculated and the experimentally obtained value is attributed to edge effects such as scattering resulting from the confined droplet at the waveguide surface.

In addition to the sensitivity improvement achieved with the single-mode GaAs waveguides, improved control on the evanescent field is prevalent for this novel waveguide structure facilitating quantitative measurements at the waveguide surface. As each individual mode propagating through a waveguide has a distinct evanescent field profile, multimode waveguides are characterized by a distribution of evanescent field intensities and profiles, which strongly depend on the coupling conditions, among other factors. A waveguide supporting only a single mode as fabricated in this study provides a well-defined evanescent field independent of the coupling conditions. Figure 5 shows a plot of the calculated relative mode intensity as a function of distance perpendicular to the direction of propagation for TM polarized light. The distance from zero in the negative direction corresponds to the radiation guided in the evanescent field. Mode profiles are shown for the single mode supported by the GaAs waveguide developed in this study, along with a high-order mode ($n = 13$) and a low-order mode ($n = 1$) for a multimode silver halide waveguide. The low-order mode profile for silver halide is very near the axis due to its low intensity

relative to the high-order mode, revealing the substantial difference in evanescent field intensities of multimode waveguides. The GaAs waveguide supports only the mode indicated by the solid line, which facilitates quantitative measurements in contrast to multimode silver halide waveguides due to a precisely defined and tunable mode structure. Furthermore, the high intensity of the evanescent mode component characteristic for the GaAs waveguide near the surface (distance of 0) compared to any mode of the silver halide waveguide is noteworthy. This allows for particularly sensitive measurements at the waveguide surface such as for monolayers of molecules. The high intensity at the waveguide surface and the sharp decay are due to the large refractive index contrast between the waveguide and the probed surface layer, as predicted by theory.

CONCLUSION

The first thin-film GaAs single-mode IR waveguides have been designed and fabricated matching the emission frequency of a DFB-QCL at $10.3 \mu\text{m}$ demonstrating MIR evanescent field liquid-phase sensing. Evanescent field absorption measurements reveal a marked increase in sensitivity in contrast to multimode silver halide waveguides, and the ability to detect acetic anhydride serving as exemplary analyte at the waveguide surface. Furthermore, these waveguides provide a well-defined evanescent field at the waveguide surface with a sharp decrease into the surrounding material rendering them ideal for sensitive and quantitative measurements of molecular monolayers deposited at the waveguide surface. These next-generation planar IR waveguides show substantial promise toward on-chip infrared chemical sensing platforms combining a single-mode-matched, thin-film waveguide ideally grown on the same substrate as the QCL for highly integrated MIR liquid-phase sensing platforms.

ACKNOWLEDGMENT

Collaboration on QCL technology with Alpes Lasers (Neuchâtel, Switzerland, www.alpeslasers.ch) is gratefully acknowledged. This work is supported in part by the National Science Foundation (NSF; Dissertation Enhancement Grant INT-O420005), and by the National Institute of Health (NIH; EB000508). The planar silver halide waveguides have been provided by Y. Raichlin and A. Katzir at Tel-Aviv University, Israel, and have been reported in a previous study.²⁰

Received for review December 15, 2005. Accepted April 11, 2006.

AC052214A